Chapter 4

Single crystallites in 'planar polycrystalline' oligothiophene films: determination of orientation and thickness by polarization microscopy

Thin films of evaporated oligothiophenes (α-nT, n = 4..8) show a "planar polycrystalline" structure: each of the individual crystallites has a random azimuthal orientation; the (a,b) face of its unit cell is aligned with the surface plane. We introduce a technique to determine the orientation and thickness of such aligned thiophene crystals by optical polarization microscopy.[(1)] As a result of the optical birefringence of the crystal, it appears with different colours in the microscope dependent on its orientation and thickness. To support the method proposed, we solve Maxwell's equations and obtain quantitative agreement with the observed colours. The organic crystal shows biaxial anisotropy. For unsubstituted quaterthiophene, α-4T, we find effective refractive indices n_b=1.84 $\pm$ 0.1 and n_a=1.61 $\pm$ 0.1 for light under normal incidence. Our conclusions are fully confirmed by Atomic Force Microscopy with molecular resolution. Our analyses result in a simple recipe to obtain the directions of the a and b crystal axes from the optical experiment.

[(1)] This work has been published by Vrijmoeth et al. [1] and forms an essential part of this thesis to characterize single crystallites for thin-film transistor applications.

4.1 Introduction

Following the pioneering work by Horowitz et al. [2], field-effect transistors based on evaporated oligothiophenes (α-nT, $n = 4..8$ monomer units) have been intensively studied [3,4]. Their special crystalline order makes these materials well suited for the study of the intrinsic charge transport properties of organic solids [3,5,6]. Under suitable preparation conditions the thiophene material crystallizes with its (a,b) crystal face aligned with the substrate plane; its molecules are almost perpendicular to the surface. This induces a "planar polycrystalline" order in the film. Each of the crystallites has its a and b axes residing within the surface plane, but has a different azimuthal orientation. Ideally, one would like to perform the study of field-effect charge transport on such a single organic crystal. It would allow to analyze the transport along both in-plane crystal axes. Further, it would rule out the influence of grain boundaries. Until now, the films prepared by vacuum evaporation have had grain sizes smaller than $\sim$0.2 μm [7]. It was only on the basis of a bulk-grown crystal that a single-crystal device has been realized [8]. Recently, however, we have obtained large single crystallites with diameters up to $\sim$25 μm of both quaterthiophene and sexithiophene by vacuum evaporation and realized transistors with such a single crystal in the active region (this thesis). To measure the mobilities along each of the crystal axes in the surface plane, one then must know their azimuthal directions. In this chapter, we introduce a simple and reliable technique to determine the directions of both in-plane crystal axes in each individual thiophene crystal by polarization microscopy [9,10]. Optical crystallography has been developed into a useful technique for the study of oriented layers [11], especially of Langmuir-Blodgett films [12]. Because of their optical birefringence, the individual crystals appear with a strong colour contrast in the microscope for different azimuthal orientations. We calculate the reflectivities solving Maxwell's equations for plane waves in the anisotropic medium. The calculations are in excellent agreement with the observed colours. The data are properly described assuming that the crystal shows biaxial anisotropy. As a result of our work, we find a simple recipe to obtain the crystal axes' directions. The thickness of the crystallite is obtained as a side product. The directions of the a and b crystal axes as obtained from the microscope coincide with those found by AFM (Atomic Force Microscopy).

We believe that our method is generally applicable to obtain the in-plane crystal orientation of birefringent materials showing the present planar polycrystalline surface ordering mode. This mode is commonly found for various materials on planar substrates, both amorphous and crystalline.

4.2 Experiment

Thin quaterthiophene films have been deposited on oxidized Si(100) substrates. The thermally grown oxide layer had a thickness in the range of 120 to 160 nm, as determined by ellipsometry. The organic films were grown by thermal evaporation from a small Ta boat in high vacuum (background pressure 10^{-7} mbar). Because of the significant desorption of the evaporant from the surface that occurs at the evaporation substrate temperature ($\sim$70 °C), the substrate was forced to cool down rapidly to room temperature (rate $\sim$0.7 °C per second) immediately following the evaporation. Further analyses were performed after the sample had been removed from the vacuum.

Average film thicknesses were determined using a Dektak surface profiler. AFM images were taken in air using a commercial instrument (Park Scientific) in contact mode.

The optical data were taken in reflection mode using a commercial high-resolution polarization microscope (Olympus BH-2). The arrangement of the polarizing elements in the optical path is sketched in Fig. 4.1 and is represented along a straight line for clarity. Angles are defined with respect to the vertical axis. Non-coherent white light with either linear or circular polarization is incident on the sample through a rotatable linear polarizer (rotation angle δ) and a $\lambda/4$ retarder plate. The sample is mounted in the microscope on a rotatable stage so that its angle of rotation α_{sample}, and that of each of the crystallites, α_c, can be varied. α_c is chosen to be the angle of the b crystal axis with respect to the vertical direction (see Fig. 4.1). The reflected light was analyzed with a linear polarizer.

With this set-up, the polarization of the incident light can be chosen to be vertical (δ=0°), circular (δ=45°) or horizontal (δ=90°). Because of the beam splitter which separates the entrance and exit beams, the optical transmission of the microscope appears to be different for horizontally and vertically polarized light. This partial polarization has been checked to be

essentially independent of wave length, and has been been taken into account in the calculations (see Section 4.2.2). The optical images were recorded using a CCD colour video camera and digitized to obtain the R, G and B colour components.

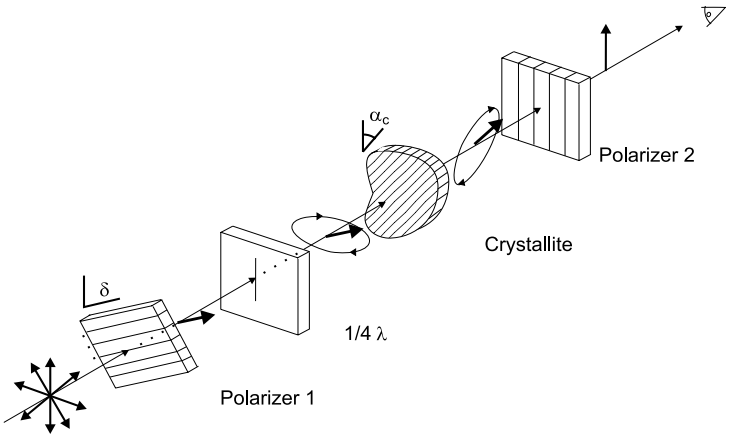

FIGURE 4.1. Set-up of the polarizing elements in the microscope. The optical path is represented by a straight line for clarity. Linearly or circularly polarized light is incident on the crystallite through a polarizer, with angle δ, and a $\lambda/4$ retarder plate. The reflected light is analyzed by a vertical linear polarizer. The angles δ and α_c of the polarizer and crystallite are defined with respect to the vertical axis, both in this figure and in the optical images.

4.2.1 Film structure: planar polycrystalline

The special planar polycrystalline ordering of the α-4T film is illustrated in Fig. 4.1. X-ray Θ-2Θ scans reproducibly reveal an ensemble of very sharp peaks (see Chapter 2), corresponding to a layering in the z-direction with 1.53 nm periodicity (Fig. 4.2(a). In addition, we have resolved terraces and steps with the same height using AFM (see Fig. 2.3). We observe this behaviour consistently for substrate temperatures between 20 and 120 °C [13].

The polycrystallinity of the film, with each of the oriented crystallites in a random azimuthal orientation, is evident in the microscope (Fig. 4.3). We find that the sizes of the individual single crystals critically depend on the preparation conditions and can become very large (diameter $\sim$25 μm) for

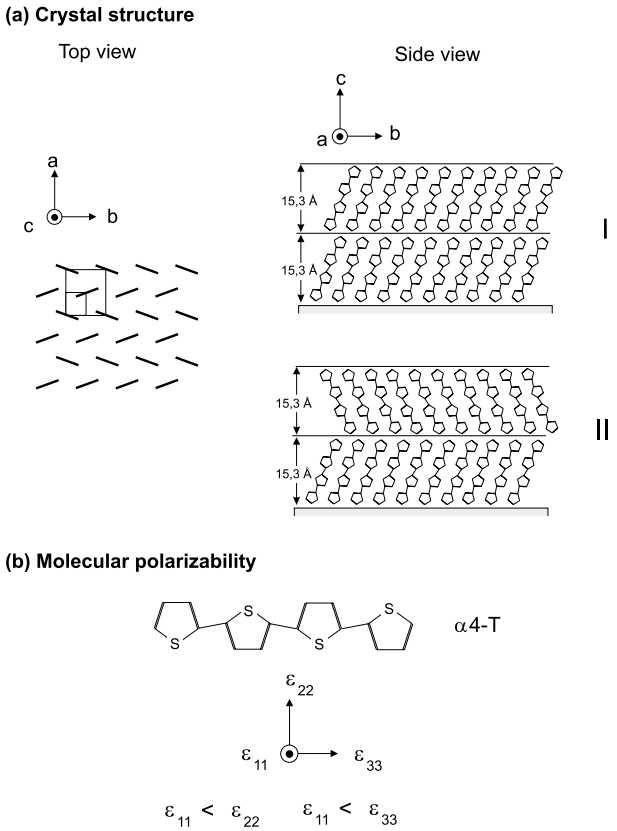

FIGURE 4.2. (a) Possible crystal structures of evaporated quaterthiophenes consistent with the layering found from Θ-2Θ X-ray data on evaporated films. (I) has been proposed on the basis of powder diffraction data [15], (II) is the structure which has been proposed for α-3T [18] and dimethyl-substituted quaterthiophene [17]. (b) Polarizability of a single α-4T molecule. The polarizability $\epsilon_{\text{crystal}}$ of the crystal is approximated by taking the average of the molecular polarizabilities in the unit cell.

optimized substrate temperatures and evaporation rates [14].

This ordering behaviour is generally found for the thiophene materials [7,15,16], with the (a,b) crystal face aligned with the surface plane, and the molecules in a herringbone arrangement. The oligomer is oriented with its molecules almost perpendicular to the substrate plane (see Fig. 4.2(a)). The detailed molecular structures occurring may show variations for the different materials.

We note that the data for quaterthiophene are consistent with two different microstructures I and II (see Fig. 4.2(a)). Either the tilt direction of the molecules is the same for each successive layer (I), or it changes over 180° azimuth for every next thiophene layer (II). Model I is supported by diffraction studies on quaterthiophene powder [15]. Structure II was found both for end-capped quaterthiophene [17], and for terthiophene [18]. These different structures also imply different optical symmetries of the crystal. On the basis of its optical behaviour, we can therefore distinguish these structures (see Section 4.4.2).

4.2.2 Optical appearance of the individual crystallites

Observation

The individual crystallites show large variations in colour in the microscope (see Fig. 4.3) for different light polarization states, thicknesses, and azimuthal orientations. These variations in colour can therefore be employed to obtain the individual orientations. We discuss these colours for different relative angles δ of the entrance and exit polarizers.

Depending on the angle δ of the entrance and exit polizers, light with different polarisation is incident on the sample. For δ=0° both polarizers are parallel resulting in light with linear polarization. For δ=45° a circularly polarized light, with δ=90° a cross polarized light is incident on the sample. The specific colour[(2)] of the crystallite is dependent on its orientation in the microscope (angle α_c), the relative angle δ and the crystal thickness.

With circularly polarized light incident on the sample, the overall colour appearance of the film changes drastically, with an enhanced contrast. One bright maximum per 180° rotation is observed (Fig. 4.3). Interestingly, this maximum in intensity does not occur for α_c=0° or α_c=90°, but for α_c=45°, independent of crystallite thickness. The absolute colour however varies with thickness.

If the incident polarizer is crossed with respect to the analyzer, the reflected intensity almost vanishes. Some light is observed for α_c=45°. The intensity is zero for α_c=0° and α_c=90°, i.e., if the polarizer and analyzer coincide with either the b or the a axis of the unit cell. This phenomenon

[(2)] All figures in this chapter are shown as black and white drawings. The more detailed colour versions of some of the figures are shown in Ref. [1].

can be employed to align the crystal accurately with the polarizers, to within $\sim 3^\circ$, by minimization of the reflected intensity. These findings can be used to develop a straightforward recipe to identify the crystal axes from the observed colour extrema. We have modelled the optical reflectance of the sample to support such a recipe.

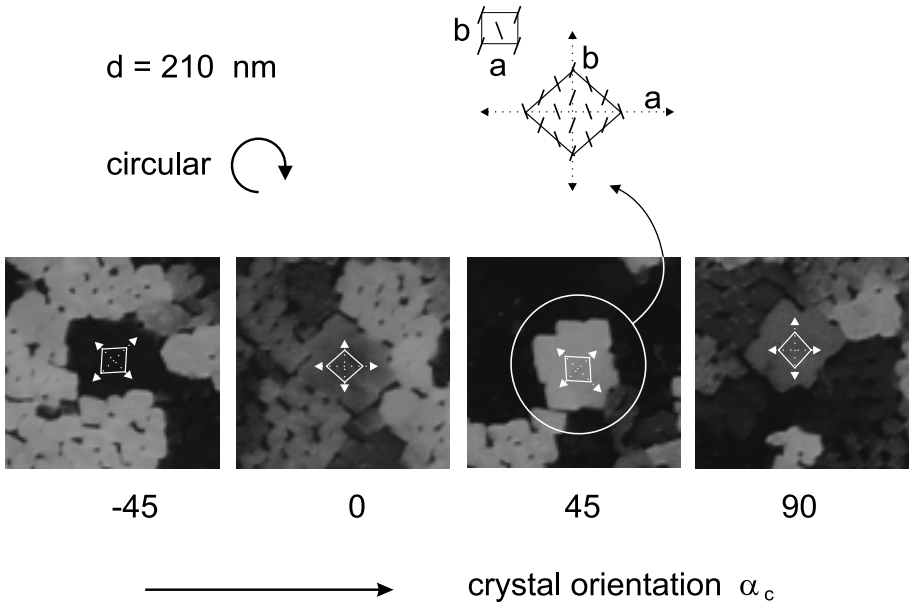

FIGURE 4.3. Appearance in the optical microscope of a single crystallite (thickness $\sim$210 nm), for different polarization states of the incident light and crystallite orientations α_c. The numbers α_c refer to the crystallite in the circle. The maximum reflected intensity for circularly polarized light is observed at $\alpha_c \sim 45^\circ$.

Model Calculation

We describe these observations in terms of the interference between light waves reflected from the crystallite surface and those from the crystallite-substrate interface. The wavelength of the light depends on its polarization direction, and this gives rise to the differences in interference colour.

We have calculated the reflectance of the thiophene-SiO_2-Si layered thin-film system to find its colours either in the optical microscope, or as seen by

the naked eye over macroscopic film areas. In the former case, we assume that the light wave is incident under a cone of angles (numerical aperture of the objective 0.9) centered around the surface normal; in the latter the light is incident along the surface normal itself.

The description of the sample reflection for both the *s*- and the *p*-polarization states (Jones matrix) requires the solution of Maxwell's equations in each of the layers of the sample (The permittivity of the thiophene film is characterized by an anisotropic tensor ϵ [19].). To that end, we have followed the approach developed by Berreman et al.[20]. The propagation of the plane waves in the z-direction, i.e., perpendicular to the interface, is described by a vector $\Psi(z)=(E_x,H_y,E_y,-H_x)$, which contains the tangential magnetic and electric field components. Within this formulation, the wave equations reduce to $d\Psi/dz=(i\omega/c)\mathbf{\Delta}\cdot\Psi$. Here, $\mathbf{\Delta}$ is the (4x4) so-called layer propagation matrix, which contains the permittivity tensor ϵ and is different for each angle of incidence. The solution to Maxwell's equations takes the form $\Psi(z)=\exp[(i\omega z/c)\mathbf{\Delta}]\cdot\Psi(0)$. Hence the wave fields at the respective interfaces, as described by $\Psi(0)$ and $\Psi(d)$, are related by

$$\Psi(d) = \exp(\frac{i\omega d}{c}\mathbf{\Delta})\cdot\Psi(0) \tag{4.1}$$

with d the crystallite thickness. The (4x4) 'layer matrix' $\exp[(i\omega d/c)\mathbf{\Delta}]$ is obtained from $\mathbf{\Delta}$ by diagonalization. The four eigenvectors of $\mathbf{\Delta}$ represent the four wave solutions that can occur in the anisotropic medium [10]. The eigenvalues are the effective refractive indices for these waves. This procedure effectively results in decomposing the incident wave field in terms of these four eigenwaves [20]. The reflectivities and transmissivities of the sample are finally obtained by matching the incident, reflected and transmitted waves at each interface, as in the standard Fresnel approach [20,21].

We have applied this method to the quaterthiophene single crystal. Its polarizability tensor $\epsilon_{\mathrm{crystal}}$ was constructed assuming that it can be approximated by averaging the contributions of the different molecules within the unit cell. The main polarizabilities $\epsilon_{\mathrm{mol,ii}}$ (i=1,2,3) of the α-4T molecules (see Fig. 4.2(b)) were assumed to be large within the molecular plane and small perpendicular to it [$\epsilon_{\mathrm{mol},22} \approx \epsilon_{\mathrm{mol},33}$, $\epsilon_{\mathrm{mol},22;33} > \epsilon_{\mathrm{mol},11}$]. The thiophene polarizabilities were assumed to be independent of wavelength. $\epsilon_{\mathrm{crystal}}$ for each of the models I and II was constructed by placing the molecules within

the unit cell and averaging their contributions to the total tensor. Note that with this approach the influence of the local field [12] is neglected.

The reflectivities and transmissivities of the SiO_2/Si interface were described by standard Fresnel coefficients. The refractive indices for Si and SiO_2 as a function of wavelength have been taken from Refs. [22] and [23]. We have carefully checked the results obtained with the present description. For instance, if one assumes a uniform polarizability tensor ϵ, the reflectivity obtained should be equal to that obtained directly from the Fresnel relations. This is indeed the case.

To describe the appearance of the crystallite in the microscope, its optical spectrum was obtained by numerically integrating its Jones matrix across the solid angle covered by the objective lens, and multiplying the resulting integrated reflectivities with the Jones matrices of the polarizing optical components.

The integration was performed by choosing different azimuthal and polar angles of incidence on a grid of concentric circles, uniformly covering the solid angle cone of the objective lens. For each specific azimuthal incident direction, the polarization direction of the incident beam was expressed within the new reference frame by transformation (we neglect polarization changes induced by the lenses). The integration mesh was chosen sufficiently small that the resulting integral was independent of mesh size [the integrand (the Jones matrix) then only shows a small variation between the mesh points].

To enable comparison with the observed colours, the calculated light spectra were finally expressed in their corresponding Red-Green-Blue (RGB) coordinates, as follows. The XYZ color coordinates were obtained from the spectra by integration using the XYZ color matching functions x_λ, y_λ, z_λ from the 1931 CIE colorimetric system ($\Delta\lambda$=5 nm) [24]. The XYZ coordinates were finally converted into RGB intensities which correspond to the RGB chromaticity coordinates of the NTSC color television system [25]. The corresponding transformation is

$$\begin{aligned} R &= 1.753X - 0.48Y - 0.265Z\,, \\ G &= -0.998X + 2.027Y - 0.029Z\,, \\ B &= 0.070 - 0.141Y + 1.072Z\,, \end{aligned} \tag{4.2}$$

from which the perceived colours expressed in their RGB colour coordinates are obtained.

Comparison with experiment

To test the predictions for the appearance of a single crystal in the microscope, we have recorded images from two α-4T single crystals with thicknesses $\sim$160 nm and $\sim$200 nm, for different sample azimuths $\alpha_{\rm sample}$ between 0 and 360°, both for 'linear' and for 'circular' light. The measured RGB colour components [26] for the 157-nm crystallite as a function of sample azimuth are shown in Fig. 4.4 (dots).

The calculations (solid lines) show good agreement with all three observed RGB components, both for 'linear' and 'circular' incident polarization (Fig. 4.4). The fits for both crystallites have been simultaneously obtained, by varying the polarizabilities of the molecules (within the molecular plane the polarizabilities were assumed uniform, i.e., $\epsilon_{\rm mol,22}$=$\epsilon_{\rm mol,33}$), the film thickness, and the crystallite orientation χ_c within the film (so that α_c=$\alpha_{\rm sample}$ +χ_c), so as to obtain a good description of the data.

For both crystal structures I and II the data are well described for $\epsilon_{\rm mol,11}$=1.83 and $\epsilon_{\rm mol,22}$=$\epsilon_{\rm mol,33}$=4.04 [27]. We note that with these molecular polarizabilities, waves under normal incidence encounter effective refractive indices of n_b=1.84 and n_a=1.61, as is found from the eigenvalues for these waves. This is in good agreement with the values obtained over macroscopic film areas. We have calculated the film colours for thicknesses between 0 and 600 nm and represented them in colour charts [1]. By careful comparison with the colours observed, using a wafer with a large variation in thickness and large crystallites, we find that these charts match the observations in detail over the thickness range from 0 to 400 nm. For thicknesses between 0 and 400 nm, the thicknesses estimated from the chart agree with those measured by a profiler scan within ± 10 nm.

4.2.3 Identification of the b and a axes in a crystallite

The data discussed in Section 4.2.2 provide an unequivocal criterion, that allows to identify the crystal axes in a simple recipe. The maximum in intensity observed for 'circular' light, δ=45° always occurs at α_c $\sim$+45°, independent of thickness. A minimum is consistently found at α_c $\sim$135° for thicknesses up to $\sim$400 nm. The resulting recipe is described in Section 4.4.1. It combines the criterion mentioned above with the colour extremes occurring along the crystal axes (α_c=0° or α_c=90°) for δ=0°. This recipe works

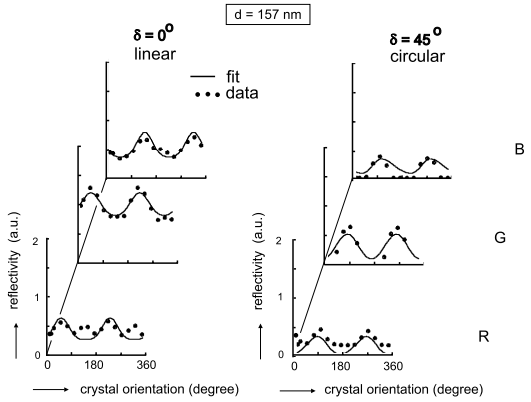

FIGURE 4.4. Observed (dots) and calculated (lines) RGB coordinates of a single crystallite (thickness 157 nm) in the microscope. This particular crystallite shows green-blue color tones. The curves have been obtained assuming molecular polarizabilities of $\epsilon_{\mathrm{mol},11}$=1.83 and $\epsilon_{\mathrm{mol},22}$=$\epsilon_{\mathrm{mol},33}$=4.04.

well for crystallite thicknesses up to ∼400 nm. Beyond that thickness, a second maximum develops at α_c=135° with 'circular' (δ=45°) light and the (δ=45° ; α_c=45°) - criterion breaks down. Therefore, in order to identify the axes in this regime one has to rely on the precise colour tones occurring. However, the (δ=0°) colour extremes still coincide with either the a or b axis, only their unequivocal identification becomes less straightforward. For these large thicknesses one runs the risk of mixing up the b with the a axes.

4.2.4 Confirmation by AFM

We finally note that the directions of the b and a crystal axes obtained agree with independent AFM measurements. The crystal orientation is reflected in the faceting shown by some of the α-4T crystallites. This faceting can be employed to check the relation between optical polarization and crystal microstructure, as the same facets are visible both in the optical microscope (Fig. 4.3) and in the AFM (Fig. 4.5)). In the latter case, we have analyzed the surface crystal lattice on top of the same island by AFM in molecular resolution (Fig. 4.5(b)). These data show the orientation of the unit cell, which has dimensions of 7.4 ± 1 and 8.4 ± 1 Å. The facets coincide with the [110] and [1$\bar{1}$0] directions in the crystal (Fig. 4.5(c)). Imaging the same crystallite in the polarization microscope, we find that the main optical axes

bisect these facet directions, as expected. The b and a axes as determined in the optical experiment coincide with those found by AFM. This completes the proof for the optical approach presented in this paper.

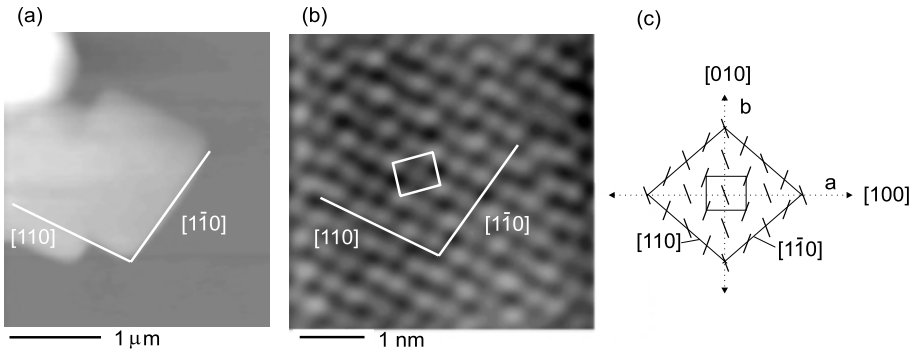

FIGURE 4.5. AFM data confirming the assignments of the crystal axes. Large area scan (a) and scan zoomed in on the same island with molecular resolution (b) show that the facet directions are [1$\bar{1}$0] and [110] directions (c), in complete agreement with the optical data. These data provide conclusive evidence for the description given in this chapter.

4.2.5 Applicability to α6-T thin films

First data on sexithiophene show that the approach presented here is directly applicable to this material as well. Films prepared at elevated substrate temperatures (~180 $\pm$ 20 °C) again show the well-known ensemble of 6 peaks in the X-ray Θ-2Θ scans, indicative of the layered crystal structure, and crystallites with diameters of ~5 - 30 μm. The colours of these crystallites in the microscope show the same general behaviour as a function of orientation in the microscope as quaterthiophene. This shows that the method developed here generally applies to these materials.

4.3 Discussion

4.3.1 Polarizability tensor

The results in this paper are represented in terms of the in-plane refractive indices n_a and n_b, for the following reason. The main unknown optical

parameter in this work is the optical polarizability of the organic crystal, as described by the general anisotropic tensor ϵ. The reflected colors, however, are almost completely determined by the polarizabilities within the surface plane, i.e., by effectively only two out of three tensor components. This is true both for the appearance of the film in the microscope and to the eye. Specifically, the film colour as apparent to the eye for light under normal incidence is expected to be completely independent of the out-of-plane optical polarizability. On the other hand, the dependence of the colours in the microscope on the out-of plane polarizabilities is also weak, as we find from our calculations. This is true even in the case of an objective with numerical aperture N.A. $\gg 1$ (large magnification), where the light waves are incident on the sample with angles of incidence which deviate significantly from the normal direction. Therefore, the out-of-surface-plane optical polarizabilities are not obtained from our experiments. Consequently, we specify the in-plane refractive indices n_a and n_b only. In practice the tensor used in the calculations has been constructed on the basis of either crystal structures I or II, assuming 'molecular' polarizabilities $\epsilon_{\mathrm{mol,ii}}$, (i = 1,2,3), such that it reproduces the experimental data (see Section 4.2.2); n_a and n_b are found as the eigenvalues of the matrix $\mathbf{\Delta}$ for normal wave incidence.

4.3.2 Wavelength dependence

Furthermore, we have neglected in our calculations a possible wavelength dependence of the polarizability. The polarizability is expected to vary especially around the main π-π^* absorption band ($\sim$580 nm). Nevertheless, the approach presented in this paper appears to work well. The refractive indices n_a and n_b from the fits represent effective refractive indices, averaged over wavelength.

4.3.3 Conclusions

A simple recipe allows to obtain the orientation and thickness of the individual organic single crystals in evaporated quaterthiophene films. The method is based on the optical birefringence of this material. To establish the method, we have solved Maxwell's equations for plane waves in the anisotropic crystal. We obtain excellent agreement with the observed

reflectances. The crystal shows biaxial anisotropy. The effective in-plane refractive indices are n_b=1.84 and n_a=1.61. The directions of the a and b crystal axes as obtained from the optical experiment are fully confirmed by AFM with molecular resolution. The present method is easily extended to other materials.

4.4 Appendices

4.4.1 Recipe to determine crystal axes

- Bring the crystallite in the center of rotation of the rotatable sample stage. Rotating the crystallite in the microscope with crossed polarizers (δ=90°), find those orientations where the reflected intensity vanishes. (This alignment can be performed with an accuracy of 3°) Here either the a or the b axes of the crystallite coincides with the analyzer, α_c=90° or α_c=0°.

- Identify the axes using circularly polarized incident light (δ=45°).

  - b-axis aligned with analyzer, α_c=0°. Rotating to positive or negative angles, the reflected intensity should increase or decrease, respectively. This corresponds to approaching the maximum at $\alpha_c \gg$45°, and the minimum at $\alpha_c \gg$315°, respectively.
  - a-axis aligned with analyzer, α_c=90°. Now the opposite happens for rotation to positive or negative angles: the intensity will decrease or increase, respectively, approaching the minimum at $\alpha_c \gg$135°, and the maximum at $\alpha_c \gg$45°, respectively.

  If the thickness is larger than ∼400 nm, a second maximum exists at α_c=135° / 315°. In that case, the identification of the a- and b axes is not straightforward.

4.4.2 Discrimination of crystal structures

Observations in the microscope provide evidence in favour of crystal structure I (see Fig. 4.2). We observe an anomalous defocusing behaviour for α-4T crystallites with crossed polarizers (α_c=45°, some intensity observed) - if the microscope is slightly defocused, each of the crystals shows an apparent

translation in the image. This translation takes place along the direction of the a axis of that particular crystal. We suggest that such a defocus-induced translation can be explained on the basis of the tilt in the optical axes that occurs for model I. The optical axes for models I and II do show a quite distinct difference in that respect. For model II, $\epsilon_{\mathrm{crystal}}$ is diagonal in the unit cell frame. For model I, this is not the case. As a consequence, for model I the optical axes are tilted with respect to the surface plane, and no longer coincide with the axis of the objective lens. Thus an asymmetry in the directions of ray propagation is introduced for model I. Therefore, we believe that our data provide support for model I, in agreement with the powder diffraction data for α-4T by Porzio et al. [15].

References

[1] J. Vrijmoeth, R.W. Stok, R. Veldman, W.A. Schoonveld, and T.M. Klapwijk, J. Appl. Phys. **83(7)**, 3816 (1998).

[2] G. Horowitz, D. Fichou, X. Peng, Z. Xu, and F. Garnier, Sol. St. Comm. **72**, 381 (1989).

[3] K. Waragai, H. Akimichi, S. Hotta, H. Kano, and H. Sakaki, Phys. Rev. B **52**, 1786 (1995).

[4] A. Dodabalapur, H.E. Katz, L. Torsi, and R.C. Haddon, Science **269**, 1560 (1995).

[5] L. Torsi, A. Dodabalapur, L.J. Rothberg, A.W.P. Fung, and H.E. Katz, Science **272**, 1462 (1996).

[6] T. Holstein, Ann. Phys. **8**, 343 (1959).

[7] A.J. Lovinger, and L.J. Rothberg, J. Mat. Res. **11**, 1581 (1996).

[8] G. Horowitz, F. Garnier, A. Yassar, R. Hajlaoui, and F. Kouki, Adv. Mat. **8**, 52 (1996).

[9] Edward Arnold, *Crystals and the polarizing microscope*, 4th edition, ltd. (London), (1970).

[10] F.D. Bloss, *an introduction to the method of optical crystallography*, Holt, Rinehart and Winston, eds. (1962).

[11] P.A. Chollet, Thin Solid Films **68**, 13 (1980).

[12] L. Servant, and M.J. Dignam, Thin Solid Films **242**, 21 (1994).

[13] For quaterthiophene the polymorphism such as that reported for sexithiophene [16] is absent for the wide temperature range studied here.

[14] Crystals with diameters of ∼25 mm are formed for a substrate temperature of 76 ± 10 °C and an evaporation rate of ∼0.6 nm/s.
[15] W. Porzio, S. Destri, M. Mascherpa, and S. Brückner, Acta Polymer. **44**, 266 (1993).
[16] B. Servet, G. Horowitz, S. Ries, O. Lagorsse, P. Alnot, A. Yassar, F. Deloffre, P. Srivastava, R. Hajlaoui, P. Lang, and F. Garnier, Chem. Mat. **6**, 1809 (1994).
[17] S. Hotta, and K. Waragai, Adv. Mat. **5**, 896 (1993).
[18] F. Van Bolhuis, H. Wijnberg, E.E. Havinga, E.W. Meijer, and E.G.J. Staring, Synth. Metals **30**, 381 (1989).
[19] The magnetic permeability μ is assumed to be unity.
[20] D.W. Berreman et al., J. Opt. Soc. Am. **62**, 502 (1972); see also D.W. Berreman, and T.J. Scheffer, Phys. Rev. Lett. **25**, 577 (1970).
[21] M. Born, and E. Wolf, "Principles of Optics", Fifth edtn., Pergamon Press, New York.
[22] D.E. Aspnes and A.A. Studna, Phys. Rev. B **27**, 985 (1983).
[23] I.H. Malitson, J. Opt. Soc. **55**, 1205 (1965).
[24] G. Wyszecki, and W.S. Stiles, "Color Science", John Wiley, New York, 1966.
[25] J. Kamler, "Luminescent Screens", Iliffe Books, London, 2nd edn., 1969.
[26] The experimental data have been obtained by integrating the reflected light over the same island area for each sample azimuth. This is realized by defining a circular area of integration from the digitized data.
[27] The polar angle of the molecules was taken to be 22°, the herringbone angle τ=36°. The film thicknesses obtained were 157 nm, and 196 nm; the orientations χ_c= 80° and χ_c= 93°, respectively.
[28] The crystals have a random azimuthal orientation with respect to the polarization of the light, as is evident from optical microscopy.